Rigid-Body Structural Mode Coupling on a Forward Swept Wing Aircraft

Gerald D. Miller,* John H. Wykes,† and Michael J. Brosnan‡
Rockwell International, El Segundo, California

Aeroelastic studies of a free-flying forward swept wing (FSW) aircraft have shown that the static aeroelastic divergence exhibited on cantilevered FSW's is replaced with a low-frequency flutter mode due to coupling between the wing divergent mode and the aircraft short-period mode. Studies of possible means of increasing this flutter speed have indicated that adding structural stiffness would result in prohibitive weight or drag penalties. An active flutter control system that employed the existing stability augmentation system of the aircraft was shown to increase the flutter speed by 40% without a performance penalty. The active flutter control system actually decreased the workload of the aircraft stability augmentation system. The coupling between the wing divergent mode and the aircraft short-period mode is also shown to have detrimental effects on flying qualities, ride qualities, and gust loads, but these effects are minimized by the active flutter control system.

Introduction and Summary

THE control of static aeroelastic divergence of forward swept wings (FSW) by the application of aeroelastic tailoring of composite structures, as first discussed by Krone,[1] has made the FSW an attractive fighter configuration. Recent studies and wind-tunnel tests by Rockwell International[2] and Grumman[3] have verified that static divergence can be controlled with a minimum weight penalty. These studies and tests have also been summarized by Hertz et al.[4] However, free-free dynamic analyses of FSW aircraft have revealed a structural dynamic instability that is more critical than static divergence. This phenomenon involves a coupling between the wing divergence mode and the aircraft short-period mode and has been called rigid-body/wing bending flutter.

The paper initially discusses the physical causes of rigid-body/wing bending flutter of FSW aircraft, followed by a study of potential solutions to this phenomenon for a Rockwell design of an FSW demonstrator (see Fig. 1). The use of active controls technology to design a flutter suppression system to control the rigid-body/wing bending flutter on Rockwell's FSW demonstrator is described, including the integration of the active system with the complete aircraft design to obtain the lightest weight structure while maintaining strength requirements, structural dynamic stability, and rigid-body stability of the aircraft. Also demonstrated are improvements in the flying qualities, ride qualities, and a reduction in the gust loads as a result of the active control system.

FSW Dynamic Analyses

Cantilevered Analyses

As emphasized in the Introduction, it is the solution to the divergence phenomenon of an FSW offered by composite structures which is the breakthrough making possible the attainment of favorable FSW attributes. It was natural, then, that initial analyses concentrated on the cantilevered wing divergence analyses.

A cantilever flutter analysis of an FSW is demonstrated in Fig. 2; shown is the wing first bending mode frequency decreasing with increasing dynamic pressure until a zero frequency static divergence instability is encountered. A cantilevered aeroelastic wind-tunnel model of a 0.6-scale FSW (Fig. 3) was built and tested by Rockwell International at the Langley 16-ft transonic dynamic wind tunnel.[2,4] The results, shown in Fig. 4, indicate that static divergence can be predicted quite adequately with state-of-the-art analysis methods. The nonlinearity of divergence dynamic pressure with load is speculated to be caused by an increase of the wing curve slope (C_{L_α}) at higher angles of attack due to the formation of a leading-edge vortex on the wing. (The increase in C_{L_α} has been found on force model test data also.)

Free-Free Analyses: Rigid-Body/Wing Bending Flutter

Surprisingly, free-free dynamic analyses of FSW aircraft have shown that static divergence is not critical. In fact, the wing response is completely different from the cantilevered case. The wing is no longer cantilevered in that it is attached to a relatively small mass fuselage which responds to the wing load and significantly modifies the cantilevered fixity condition. As seen in Fig. 5, the wing first bending mode frequency begins to drop with increasing dynamic pressure, but the aircraft short-period mode frequency rises with increasing dynamic pressure. The short-period mode couples with the wing divergence-prone mode, resulting in flutter at a speed lower than the static divergence speed. It is interesting to note that not only is static divergence not critical in the case shown in Fig. 5, but also it no longer exists.

Rigid-body/wing bending flutter, a phenomenon involving the coupling between a structurally divergence-prone mode and an aircraft rigid-body mode, is not a newly discovered phenomenon. Early design analyses of the XB-70 by Wykes and Lawrence[5] showed a rigid-body coupling flutter mode resulting from the long forward fuselage/canard combination having divergence tendencies and coupling with the rigid-body short-period mode. Also, aeroelastic analyses of oblique-wing aircraft by Jones and Nisbet[6] and by Weisshaar and Crittenden[7] demonstrated that the mode of instability changed from static divergence to flutter when the wing was allowed rigid-body roll freedom.

On FSW aircraft, a close analogy can be drawn between rigid-body/wing bending flutter and classical bending/torsion flutter. As shown in Fig. 6, classical bending/torsion flutter occurs as a result of the coupling between properly phased bending and torsion modes when the relative frequencies of the two modes are close together. For typical aft swept wings (ASW), the bending mode rises in frequency and the torsion

Presented as Paper 82-0683 at the AIAA/ASME/AHS 23rd Structures, Structural Dynamics and Materials Conference, New Orleans, La., May 10-12, 1982; submitted May 28, 1982; revision received Dec. 17, 1982.

*Member of Technical Staff, North American Aircraft Operations. Member AIAA.

†Member of Technical Staff. North American Aircraft Operations. Associate Fellow AIAA.

‡Member of Technical Staff. North American Aircraft Operations. Member AIAA.

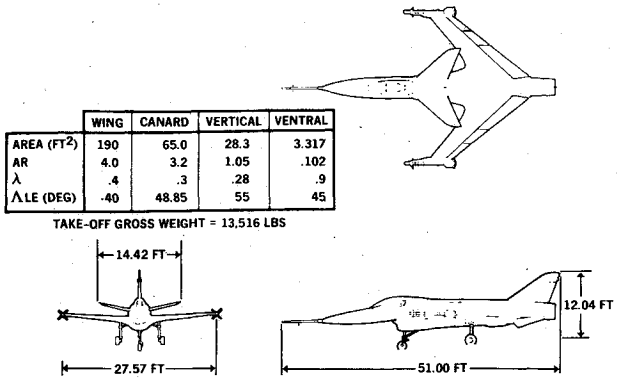

Fig. 1 General characteristics of Rockwell International FSW demonstrator.

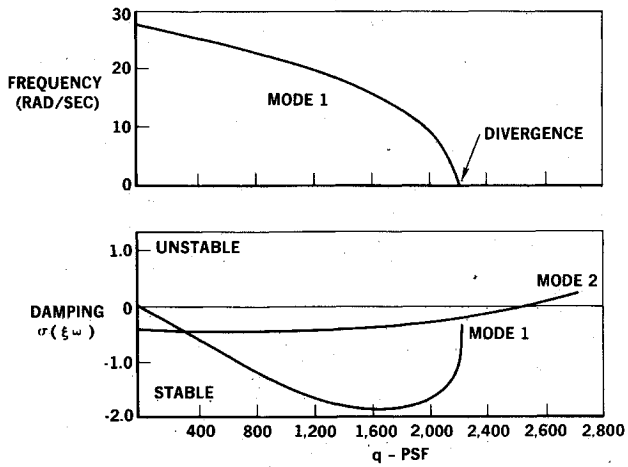

Fig. 2 Example of FSW cantilevered flutter analysis results.

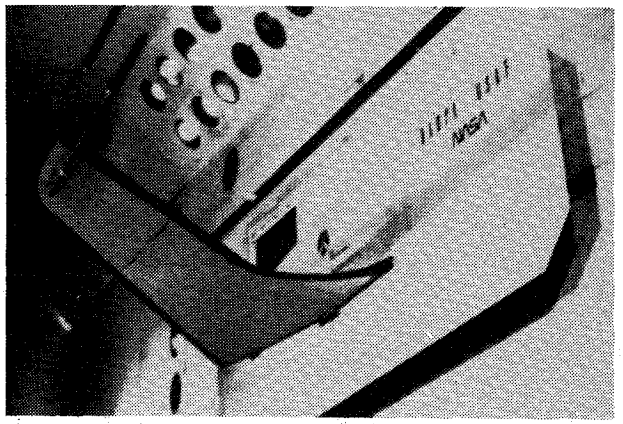

Fig. 3 FSW cantilever flutter model test.

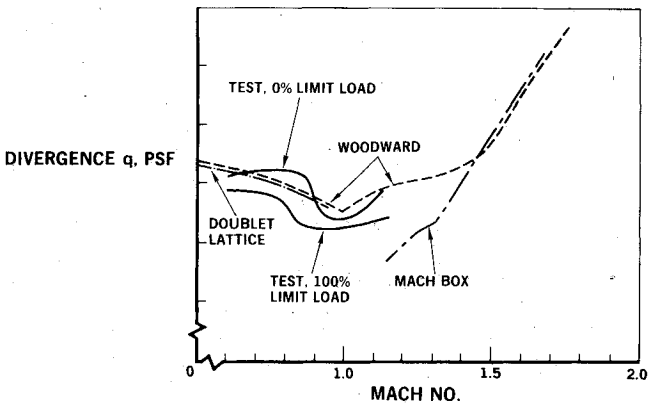

Fig. 4 Cantilevered wing divergence results.

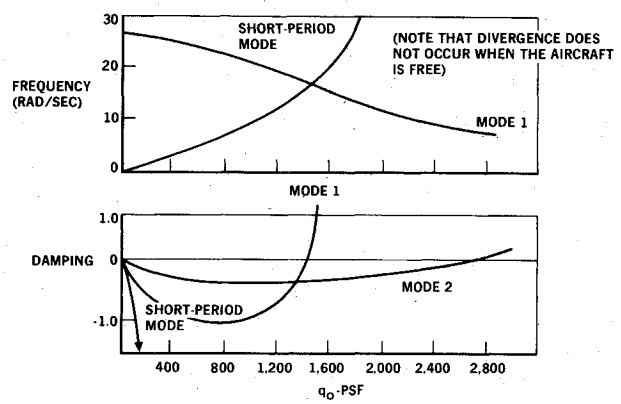

Fig. 5 Example of FSW free-free flutter analysis results.

mode drops in frequency with increasing speed, causing the frequencies of the two modes to come together. On FSW, the bending and torsion modes both drop in frequency with increasing speed and may not converge, a result which has led many people to speculate that an FSW would not be subject to bending/torsion flutter. Flutter-producing phasing consists of the torsion mode producing a force that is in phase with the wing bending velocity. Rigid-body/wing bending flutter occurs as a result of coupling between properly phased wing bending and the aircraft rigid-body pitching mode when the frequencies of the two modes are close together. For typical FSW's, the bending mode drops in frequency and the aircraft short-period mode rises in frequency with increasing speed, causing the frequencies of the two modes to come together. To obtain the proper phasing for rigid-body/wing bending flutter, the force on the wing bending mode due to the rigid-body pitching mode must be in phase with the wing bending velocity.

Understanding the analogy between bending/torsion flutter and rigid-body/wing bending flutter, and using a well-known fact that mass ballast (either forward or aft) on a wing can change the phasing between the bending and torsion modes enough to eliminate flutter, an attempt was made to adjust the FSW fuselage mass distribution to change the phasing between the wing bending and aircraft short-period modes in an analytical study. Understanding how fuselage mass distribution can change the phasing between the two modes can be seen by considering the motion of the aircraft undergoing free natural vibration motion. When the wing is undergoing a natural bending motion, a pitching moment is created about the aircraft center of mass because the wing center of mass is either forward or aft of the aircraft center of mass. In free vibration modes, angular momentum must be equal to zero. Thus, the free fuselage rotates in such a way that an angular moment is produced which opposes that of the wing bending motion, resulting in zero angular momentum. This effect is shown by the two examples in Fig. 7. The first shows an FSW aircraft with the wing center of mass aft of the aircraft center of mass, and the second shows the wing center of mass forward of the aircraft center of mass. The phase diagrams show the relative magnitudes of the displacements and aerodynamic forces for the wing bending mode η_j and the aircraft pitching and plunging motion, θ and h, taken from a flutter analysis. For each case, the wing bending motion has been normalized along the right-hand axis. It is seen that there is a phase shift of approximately 180 deg in the aircraft pitching motion between the two cases, as would be expected. The interesting result, however, is the phasing and magnitude of the associated aerodynamic coupling force on the wing due to aircraft pitch $F\eta_j\theta$. In the case where the wing center of mass is aft, the coupling force is relatively large and almost

Table 1 Results of study of fixes for rigid-body/wing bending flutter

Configuration	Performance goals effect	Drag count, $M = 1.2$	Flutter speed factor[a]
Reduce sweep 5 deg, $\Lambda = 35$ deg	+ 8-9 s accel time	+ 60	1.037
Reduce sweep 10 deg, $\Lambda = 30$ deg	+ 16-20 s accel time	+ 120	1.103
Increase t/c to 6%	+ 7-8 s accel time	+ 40	1.200
Increase t/c to 5.5%	+ 5-6 s accel time	+ 27	1.100
t/c root = 5%, t/c tip = 6%	+ 5-6 s accel time	+ 27	1.057
Increase λ to 0.45	Weight increase	—	1.019
Increase λ to 0.35	More difficult airfoil design	—	1.000
Increase wing skin thickness			
50 lb per aircraft	Small	0	1.040
125 lb per aircraft	Small	0	1.088
High modulus composites	Negl.	0	1.170
SAS enhancement (SASE)	None	0	1.400

[a] Target flutter speed factor = 1.35.

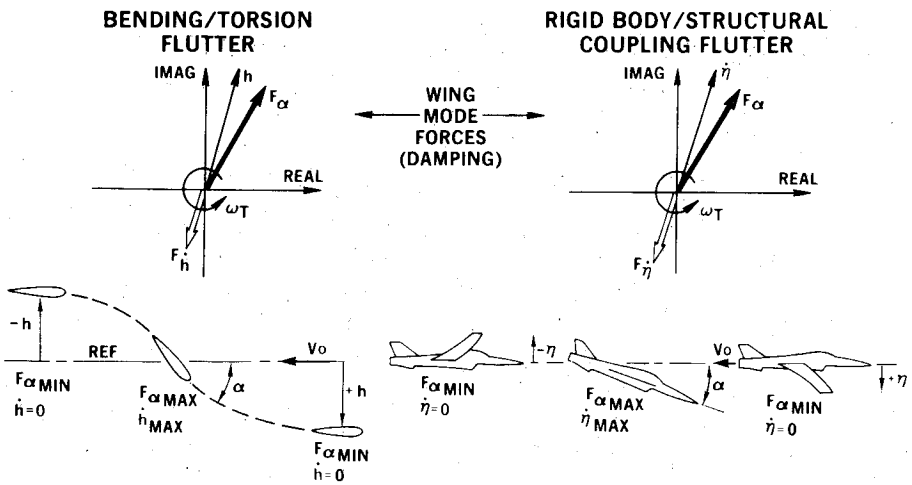

Fig. 6 Analogy of rigid-body/wing bending flutter to classical wing bending/torsion flutter.

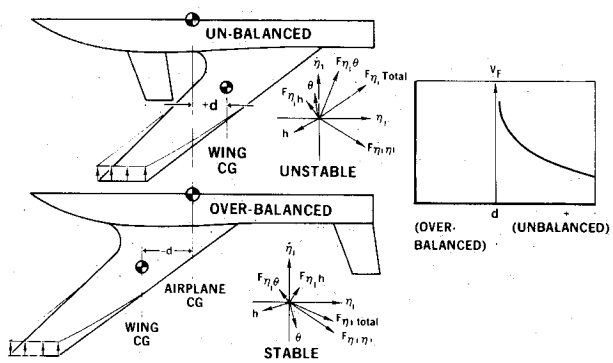

Fig. 7 Rigid-body/wing bending flutter dependency on relationship between wing and aircraft centers of gravity.

directly in phase with the wing bending velocity. This force is large enough to overcome the wing natural damping force $F_{\eta_1\eta_1}$, and causes the wing mode to be unstable. In the case with the wing center of mass forward, the coupling force has shifted by approximately 60 deg (still in phase with the wing velocity), but has been considerably reduced in magnitude and is no longer large enough to overcome the wing's damping force, allowing the wing to remain stable.

Also in Fig. 7 is a curve showing rigid-body/wing bending flutter speed vs the distance between the wing center of mass and the aircraft center of mass for a typical FSW aircraft. As the wing center of mass is moved forward from an aft position approaching the aircraft center of mass, the flutter speed increases to an infinite value. When the wing center of mass is in line or forward of the aircraft's, rigid body coupling flutter no longer occurs. The aerodynamic static stability was held constant during these analyses.

A Study of Potential Fixes

A study of possible solutions to rigid-body/wing bending flutter on a Rockwell-designed FSW demonstrator aircraft was conducted. It was determined that to rid the aircraft of rigid-body/wing bending flutter by moving the relative positions of the wing and aircraft center of masses would cause too drastic a change in the aircraft configuration; therefore, this was not considered. Other structural and configuration changes considered were reducing wing sweep, increasing wing skin thickness, changing wing taper ratio, or using higher modulus composite material. Table 1 shows the effect that these changes had on flutter speed, together with their associated effect on the aircraft performance. It is seen that, in order to obtain the required flutter speed, a combination of structural and configuration changes would have

been required, resulting in a significant degradation in aircraft performance.

A study was also conducted to determine the possibility of employing the active controls on the wing surface, which were an existing part of the aircraft stability augmentation system (SAS), to control the rigid-body coupling flutter. As shown in Table 1, this could give the entire increase in flutter speed desired without adverse effects on the aircraft performance.

Active Flutter Suppression or "SAS Enhancement"

Rationale for Active Control Solution

A decision was made to use the active controls on the wing to suppress the rigid-body/wing bending flutter for the following reasons:

1) There would be no impact on the aircraft's configuration and its performance.

2) The frequency of the rigid-body/wing bending flutter was low (approximately 3 Hz) and in the same range where the SAS system operated. Thus, the existing control surfaces and actuator designs could be employed without modification.

3) The FSW configuration was an ideal candidate for such a system because the aileron surface (which would be used to damp the wing motion) is very close to the aircraft's center of mass (see Fig. 10). Thus, the system could operate without adversely affecting the operation of SAS. In fact, the system was found actually to reduce the workload of SAS. An additionally significant fact is that the outboard control surface effectiveness increases with dynamic pressure (opposite to the loss of effectiveness on aft swept wings).

4) The feasibility of the system was shown by preliminary analysis, backed by actual experience with similar systems on the XB-70 and the B-1 aircraft.

5) The system, although primarily designed for flutter suppression, improved the flying quality and ride quality of the aircraft and also reduced the design gust loads on the wing. It was for these reasons that the system was named "SAS Enhancement," or SASE.

Some Aeroelastic Considerations

Before proceeding to the details of the SASE system design, a brief digression is made into the area of aeroelasticity of forward swept wings. A convenient way to view aeroelastic characteristics is in the form of flexible-to-rigid ratios of primary stability and control derivatives. In doing this for the FSW, it became immediately apparent that there were significant trend differences between FSW and ASW configurations. These differences were important in the developing of the SASE design. In some of the key figures to follow, the actual FSW will be contrasted with typical ASW data.

The flexible-to-rigid ratio data displayed herein were developed using modal data. Such data automatically reflect both aerodynamic and inertial loadings. The data are for $M=0.90$.

In Fig. 8, the entire vehicle normal force curve slope (C_{N_α}) flexible-to-rigid ratio is displayed. A significant increase of C_{N_α} for the FSW with increasing dynamic pressure is shown, as was expected due to the wing's divergence tendency. The increase at the maximum flight dynamic pressure is quite significant and impacts the vehicle's dynamic characteristics in the areas of handling and ride qualities, as will be discussed subsequently. In contrast, note the typical ASW C_{N_α} drop-off with increasing dynamic pressure.

The outboard control surface normal force effectiveness ($C_{N_{\delta OA}}$) and pitching moment effectiveness ($C_{M_{\delta OA}}$) flexible-to-rigid ratio data are presented in Fig. 9. Note that an outboard control surface on an ASW tends to lose its effectiveness rapidly with increasing dynamic pressure, and many times actually reverses the force effectiveness at high dynamic pressures. In marked contrast, and of particular significance to the active control of flutter solution proposed,

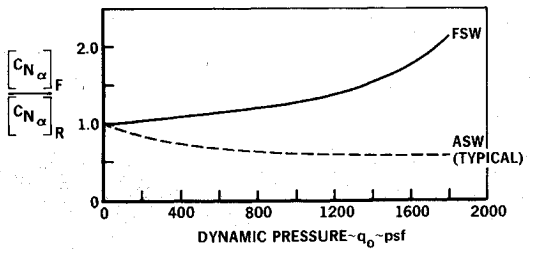

Fig. 8 Normal force curve flexible-to-rigid ratio, $M=0.90$.

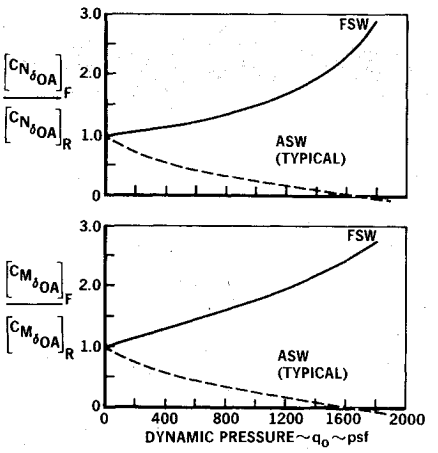

Fig. 9 Outboard control surface normal force and pitching moment effectiveness flexible-to-rigid ratios, $M=0.90$.

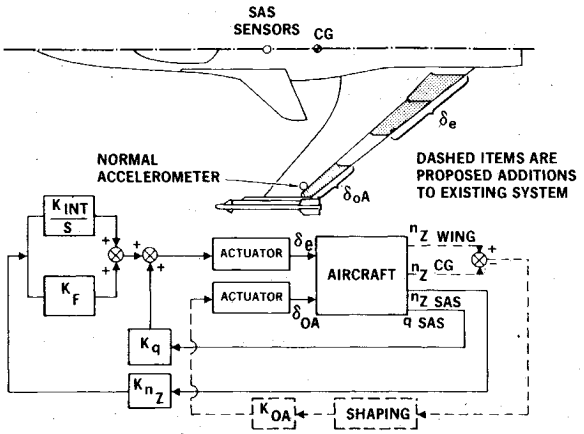

Fig. 10 General arrangement of pitch SAS enhancement (SASE).

is the fact that on the FSW the force effectiveness remains high at high dynamic pressures.

SASE System Design

Figure 10 shows the control surfaces and sensors used for the SAS and SASE, along with a block diagram of the systems. The outboard ailerons are activated by a sensor near the surfaces, thus employing the ILAF (identically located accelerometer and force) principle of Wykes and Mori[8] to assure that other wing modes would not be driven unstable. It should be noted that the acceleration at the aircraft center of mass is subtracted from that on the wing, leaving only a wing response signal in the SASE loop. The frequency response of the closed-loop SASE system at the V_L design condition, with a compensation in the feedback loop of unity, is shown in a Nyquist plot on Fig. 11a. It can be seen that a phase lag of approximately 125 deg would be required to stabilize mode 1. Figure 11b shows the system with a compensation of $[10/(S+10)]^2$ in the feedback loop. This compensation,

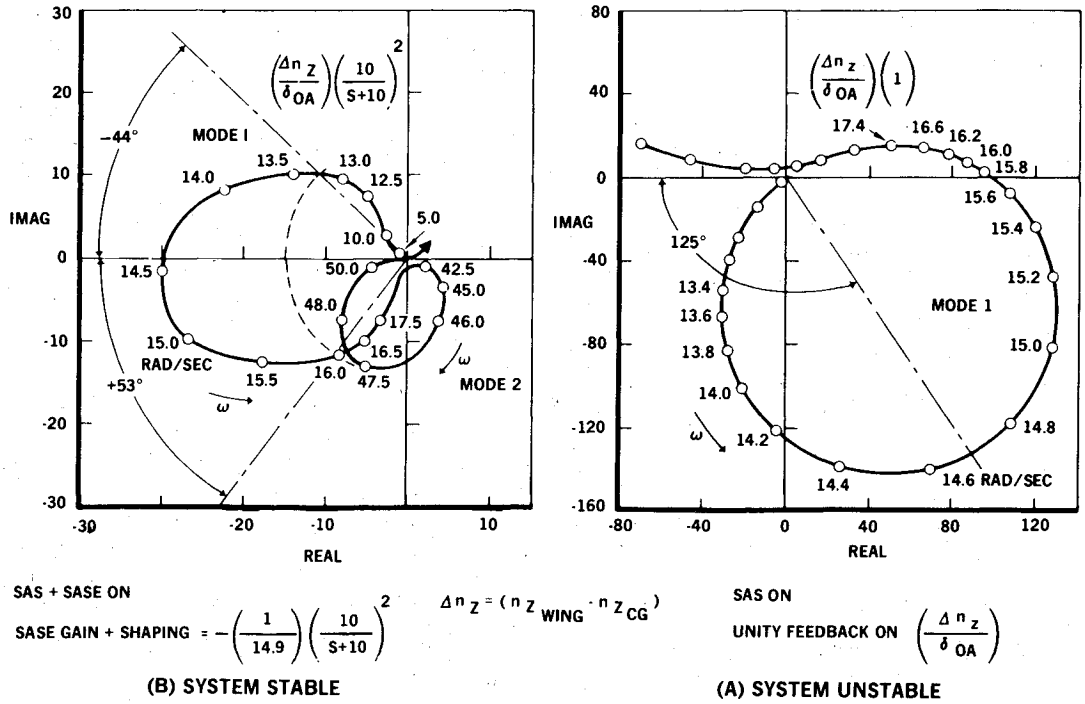

Fig. 11 Nyquist plots for SASE design, SAS on at V_L design condition ($M = 1.2$, alt = 5000 ft, $q_0 = 1775$ psf).

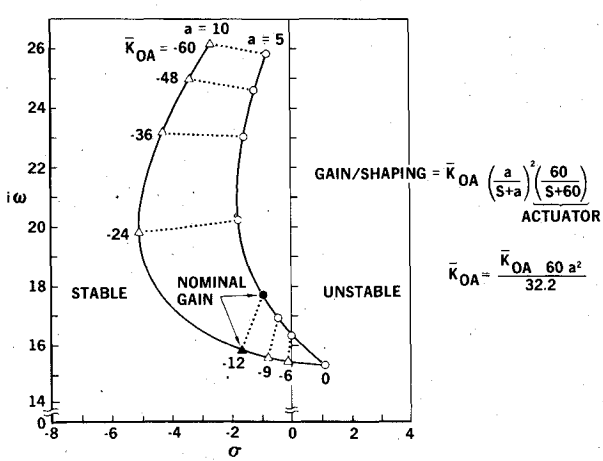

Fig. 12 SASE gain and shaping effects on mode 1 frequency and damping, SAS on ($M = 1.2$, alt = 5000 ft, $q_0 = 1775$ psf).

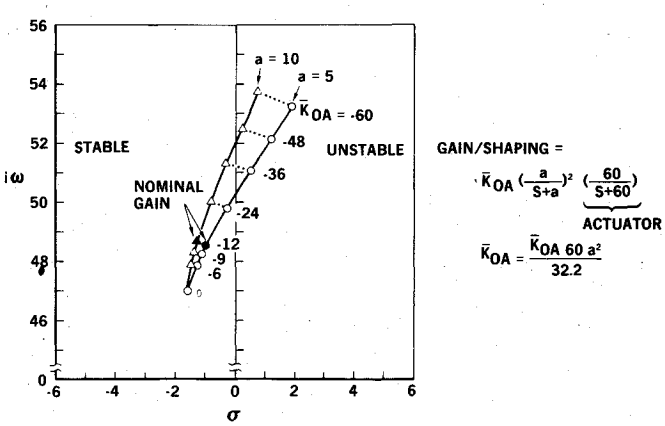

Fig. 13 SASE gain and shaping effects on mode 2 frequency and damping, SAS on ($M = 1.2$, alt = 5000 ft, $q_0 = 1775$ psf).

when coupled with the rest of the system, produces the required phase lag of 125 deg. It is seen that mode 1 has been stabilized. (Stabilized modes circle the -1.0 point on the Nyquist plot in the counterclockwise direction.) The proper gain level is picked to put the -1.0 point in the center of the circle created by the response of mode 1.

An alternate method employed to fine-tune the system compensation and gain is to plot root loci plots of the various modes for variable phase and gain levels. Figures 12 and 13 show the responses of modes 1 and 2 for compensation of $[5/(S+5)]^2$ and $[10/(S+10)]^2$ for various gain values. These plots quickly show the advantages of one phase level over another. Curve-fitted unsteady aerodynamics in the S plane (Laplace) were used in these analyses.

SASE System Design Criteria

In assembling the following criteria for SASE, attention was given to MIL-F-9490D, "General Specification for Flight Control System for Piloted Military Aircraft," and to the experience of others in designing active controls for stabilizing structural modes. In particular, Boeing's criterion in designing such a system for the B-52 CCV aircraft was considered.

Boeing's criteria indicate that, for the B-52 CCV active flutter suppression system, the design gust (no rate or deflection limiting) was 13 ft/s rms. Furthermore, the system was required to be stable in turbulence having a probability of occurrence of 10^{-6}. This latter requirement led to the analytical exposure of the aircraft and control systems to turbulence having an intensity of 32 ft/s rms. These analyses were designed to define the rate and deflection limits of the control surface which could be permitted without encountering instabilities due to nonlinearities. These requirements are very severe. It is believed that a design gust for the FSW fighter of 10 ft/s rms would be more appropriate in light of the demonstration nature of the aircraft. The maximum gust to test for instabilities due to the rate and deflection limiting was selected as having a probability of 10^{-5}. Although this is less severe than the B-52 requirement, it is considered adequate and is compatible with the MIL-F-9490D requirement for mission-essential control systems. Since V_L is the maximum flight or design speed for the aircraft, these gust requirements were applied at this speed.

The gain and phase margins of ± 6.0 db and ± 45 deg, respectively, have been chosen as appropriate for application to the critical structural modes to be stabilized. These

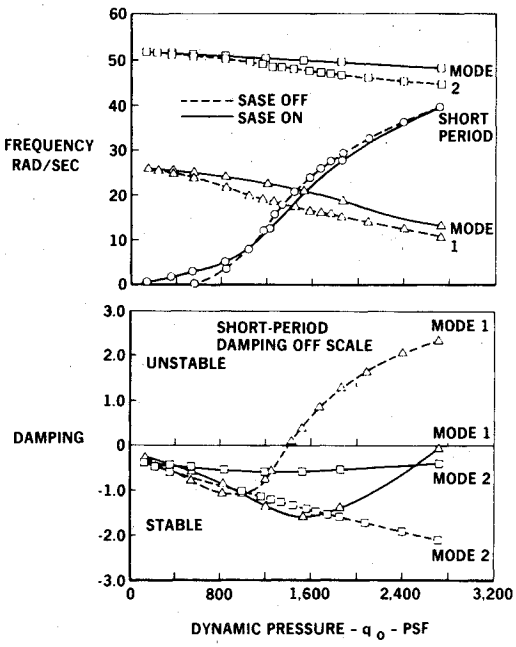

Fig. 14 SASE performance in controlling critical symmetric flutter modes, SAS on, $M = 0.90$ aerodynamics.

requirements are applicable at speeds up to V_L. These requirements are consistent with MIL-F-9490D specifications.

The SASE design criteria for flutter suppression may be summarized as follows:

1) The design gust for the SASE is 10 ft/s rms; however, the SASE must demonstrate stability in a gust environment having a probability of exceedance of 10^{-5}. (Refer to MIL-F-9490D, Table V.) These gusts will be applied at V_L.

2) For the SASE operational envelope up to V_L, gain margins are ±6.0 db and phase margins are ±45 deg on critical structural modes.

3) The SASE is at least neutrally stable at $1.15V_L$ at nominal phase and gain (gain margin 0, phase margin 0).

SASE System Performance

The ability of the SASE system to increase the rigid-body/wing bending flutter speed is shown in Fig. 14 on frequency and damping vs dynamic pressure plots. The flutter dynamic pressure has been doubled by the active control system. The effect that the SASE system has on other structural modes and the aircraft short-period mode is shown in Table 2. The table lists the frequencies and dampings for the aircraft short-period mode, along with the first 10 structural modes at the highest dynamic pressure point in the flight envelope for two different SASE compensations. It is seen that, although the unstable wing mode has been stabilized, very little change has occurred in the other modes in the system, except for mode 2, which has somewhat lower damping. The workload of the SAS and SASE system is demonstrated in Fig. 15 for four flight conditions along V_L, at a Mach number range of 0.9-1.40. Figure 15 shows the deflections and deflection rates due to a 10-ft/s rms gust. A significant result is that the application of SASE actually reduces the workload of the SAS system while doing its primary job of stabilizing the wing first bending mode.

Rigid-Body Coupling and Its Effects other than Flutter

The rigid-body coupling phenomenon, occurring in the low-frequency range near the aircraft short-period mode, also affects the flying and ride quality of the aircraft. These associated effects of rigid body coupling should be expected because the wing mode has a very large flexible-to-rigid lifting force (the increase in rigid-body aerodynamic force associated with the flexibility of a structural mode) at moderate dynamic pressures due to its divergence tendencies, as illustrated in Fig. 9. Therefore, even when the wing mode is dynamically stable, the coupling effects are large enough to create very undesirable flying and ride qualities of the aircraft.

However, the application of the SASE system, which adds damping to the wing mode, can greatly improve the aircraft's flying quality and moderately improve the aircraft's ride quality. Figure 16 shows the effect of the FSW aircraft longitudinal response due to a discrete gust. It is seen that the rigid aircraft, with SAS only operating, has very desirable damping. However, the effect of structural flexibility greatly

Table 2 Effect of SASE on mode roots, SAS on [$M = 1.2$, alt = 5000 ft, $q_0 = 1775$ psf (V_L)]

Mode	SASE gain 0	Roots,[a] $\sigma + i\omega$ SASE gain[b] Nominal (−12.48)	SASE gain[c] Nominal (−12.48)
Short	−16.55	−16.94	−16.59
period	+*i*27.87	+*i*26.72	+*i*26.34
1	+1.12	−0.91	−1.57
	+*i*15.25	+*i*17.65	+*i*15.79
2	−1.54	−0.94	−1.23
	+*i*47.19	+*i*48.53	+*i*48.60
3	−3.81	−3.86	−3.86
	+*i*102.23	+*i*102.28	+*i*102.28
4	−0.65	−0.64	−0.64
	+*i*125.69	+*i*125.68	+*i*125.68
5	−8.64	−8.51	−8.58
	+*i*131.55	+*i*131.59	+*i*131.59
6	−7.23	−7.03	−7.03
	+*i*141.48	+*i*141.49	+*i*141.50
7	−18.13	−17.92	−17.92
	+*i*180.07	+*i*180.01	+*i*180.02
8	−2.58	−2.58	−2.58
	+*i*259.22	+*i*259.22	+*i*259.22
9	−27.54	−27.53	−27.53
	+*i*261.84	+*i*261.85	+*i*261.86
10	−8.60	−8.56	−8.56
	+*i*343.34	+*i*343.40	+*i*343.40

[a] σ = damping; ω = frequency, rad/s. [b] Shaping = $[5/(S+5)]^2$. [c] Shaping = $[10/(S+10)]^2$.

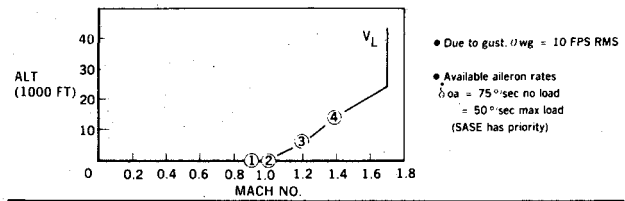

	FLIGHT CONDITION	CONTROL SYSTEM	$\dot{\delta}_e$ DEG/SEC	δ_e DEG	$\dot{\delta}_{oa}$ DEG/SEC	δ_{oA} DEG
1	M .90 AT S.L. •	SAS	40.7	2.76	—	—
	q_o 1200 psf	SAS · SASE	37.4	2.59	15.9	.87
2	M 1.0 AT S.L. •	SAS	83.6	5.45	—	—
	q_o 1500 psf	SAS · SASE	65.4	3.87	27.5	1.63
3	M 1.2 AT 5K •	SAS	66.2	4.68	—	—
	q_o 1775 PSF	SAS · SASE	45.3	3.20	53.7	3.33
4	M 1.4 AT 13K ••	SAS	44.2	2.75	—	—
	q_o 1775 PSF	SAS · SASE	32.5	2.16	19.4	1.12

*Using M = .90 doublet lattice unsteady aero
**Using M = 1.40 Woodward quasisteady aero

Fig. 15 Summary of SAS/SASE control surface rates and deflections.

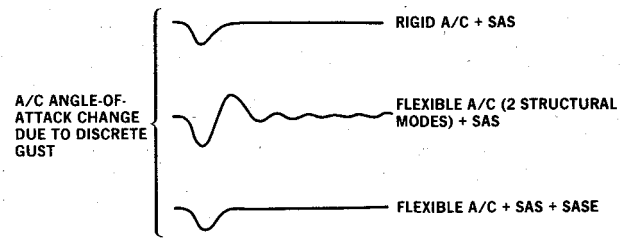

Fig. 16 Effect of SAS on flying qualities at $M = 0.90$, sea level.

σ_{wg} = 10 FT/SEC RMS

	$\bar{H}_Z$	$\dot{\delta}_e$ (DEG/SEC)	δ_e (DEG)	$\dot{\delta}_{oA}$ (DEG/SEC)	δ_{oA} (DEG)
SAS (RIGID A/C)	0.091	25.6	1.37	-	-
SAS	0.104	40.7	2.76	-	-
SAS + SASE+ (-3.75)	.099	37.4	2.59	15.98	.87
SAS +SASE* (-12.34)	.092	33.7	2.46	34.40	1.77

+ SHAPING $\left(\frac{5}{S+5}\right)^2$
* SHAPING $\left(\frac{10}{S+10}\right)^2$

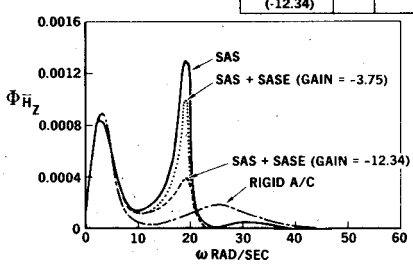

Fig. 17 Ride quality and control surface activity, SAS off/on, at $M = 0.90$, sea level ($q_0 = 1200$ psf).

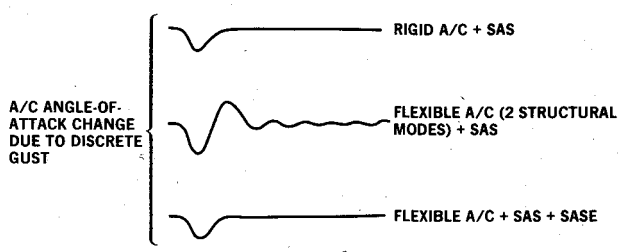

Fig. 18 Effect of SASE on wing gust loads.

reduces the damping. The effect of adding SASE greatly increases the damping of the aircraft, creating a response much like that of the rigid aircraft.

The effect of the ride quality of the aircraft is shown in Fig. 17. The figure shows a plot of the power spectral density of the ride quality parameter[9] $\bar{H}_Z$ in the vertical acceleration direction for the flight conditions of $M = 0.90$ at sea level. It is seen that the rigid aircraft's response is much less than that of the flexible aircraft with SAS only. However, the application of SASE, shown at two different gain levels, has significantly reduced the response near the frequency where the rigid-body coupling occurs, thus tending to improve the ride quality of the aircraft to nearly that of the rigid vehicle.

Also, because of the rigid-body coupling phenomenon, the wing loads due to gust are increased. However, the application of SASE, as shown in Fig. 18, reduces the wing bending moment due to gusts from a critical design parameter to noncritical levels.

Conclusion

Structural dynamic analyses of FSW aircraft have shown that aeroelastic divergence is not critical, but that a phenomenon called rigid-body/wing bending flutter is critical for certain aircraft configurations. A dominant variable causing the phenomenon, in addition to wing sweep, is the inertial coupling between the wing and the rest of the aircraft. Also associated with the coupling phenomenon is a significant degradation in the aircraft flying qualities and ride qualities and increased wing gust loads. However, by employing active controls technology, the ability to suppress the rigid-body/wing bending flutter, improve flying qualities and ride qualities, and reduce wing gust loads has been demonstrated by the analyses.

References

[1] Krone, N.J. Jr., "Divergence Elimination With Advanced Composites," AIAA Paper 75-1009, Aug. 1975.

[2] Ellis, J.W., Dobbs, S.K., and Miller, G.D., "Structural Design and Wind Tunnel Testing of a Forward Swept Fighter Wing," AFWAL-TR-80-3073, July 1980.

[3] Wilkinson, K. and Rauch, F., "Predicted and Measured Divergence Speeds of an Advanced Composite Forward Swept Wing Model," AFWAL-TR-80-3059, July 1980.

[4] Hertz, T.J., Shirk, M.H., Ricketts, R.H., and Weisshaar, T.A., "On the Track of Practical Forward-Swept Wings," *Astronautics & Aeronautics*, Vol. 20, Jan. 1982, p. 40-52.

[5] Wykes, J.H. and Lawrence, R.E., "Aerothermoelasticity: Its Impact on Stability and Control of Winged Aerospace Vehicles," *Journal of Aircraft*, Vol. 2, Nov.-Dec. 1965, p. 517-526.

[6] Jones, R.T. and Nisbeth, J.W., "Aeroelastic Stability and Control of an Oblique Wing," *The Aeronautical Journal of the Royal Aeronautical Society*, Vol. 80, Aug. 1976.

[7] Weisshaar, T.A. and Crittenden, J.B., "Flutter of Asymmetrically Swept Wings," *AIAA Journal*, Vol. 14, Aug. 1976, p. 993-994.

[8] Wykes, J.H. and Mori, A.S., "An Analysis of Flexible Aircraft Structural Mode Control," AFFDL-TR-65-190, Pt. I, June 1966.

[9] Rustenburg, J.W., "Development of Tracking Error Frequency Response Functions and Aircraft Ride Quality Design Criteria for Vertical and Lateral Vibration," ASD-TR-7-18, Jan. 1971.